Pulse energy dependence of subcellular dissection by femtosecond laser pulses

A. Heisterkamp[*], I. Z. Maxwell, E. Mazur

Department of Engineering and Applied Science, Harvard University, Cambridge, MA 02138
[*]now with: Laser Zentrum Hannover, Hannover, D-30419, Germany
ah@lzh.de mazur@physics.harvard.edu

J. M. Underwood, J. A. Nickerson

Department of Cell Biology, University of Massachusetts, Worcester, MA 01655

S. Kumar, D. E. Ingber

Vascular Biology Program, Departments of Pathology and Surgery, Children's Hospital Boston and Harvard Medical School, Boston, MA 02115

Abstract: Precise dissection of cells with ultrashort laser pulses requires a clear understanding of how the onset and extent of ablation (i.e., the removal of material) depends on pulse energy. We carried out a systematic study of the energy dependence of the plasma-mediated ablation of fluorescently-labeled subcellular structures in the cytoskeleton and nuclei of fixed endothelial cells using femtosecond, near-infrared laser pulses focused through a high-numerical aperture objective lens (1.4 NA). We find that the energy threshold for photobleaching lies between 0.9 and 1.7 nJ. By comparing the changes in fluorescence with the actual material loss determined by electron microscopy, we find that the threshold for true material ablation is about 20% higher than the photobleaching threshold. This information makes it possible to use the fluorescence to determine the onset of true material ablation without resorting to electron microscopy. We confirm the precision of this technique by severing a single microtubule without disrupting the neighboring microtubules, less than 1 μm away.

OCIS codes: (170.0180) Medical optics and biotechnology; (140.7090) Ultrafast lasers; (180.2520) Fluorescence microscopy

References and links

1. W. Denk, J.H. Strickler, and W.W. Webb, "Two-Photon Laser Scanning Fluorescence Microscopy," Science **248**, 4951, 73-76 (1990)
2. K. Koenig, "Multiphoton Microscopy in Life Sciences," J. Microscopy **200**, 83-104 (2000)
3. D. Stern, R.W. Schoenlein, C.A. Puliafito, E.T. Dobi, R. Birngruber, and J.G. Fujimoto, "Ablation by Nanosecond, Picosecond, and Femtosecond Lasers at 532 nm and 625 nm," Arch. Ophthalmol. **107**, 587-592 (1989)
4. P.T.C. So, H. Kim, and I.E. Kochevar, "Two-photon deep tissue ex vivo imaging of mouse dermal and subcutaneous structures," Opt. Express **3,** 339-350 (1998), http://www.opticsexpress.org/abstract.cfm?URI=OPEX-3-9-339
5. N. Shen, C.B. Schaffer, D. Datta, and E. Mazur, "Photodisruption in biological tissues and single cells using femtosecond laser pulses," in *Lasers and Electro Optics*, conference technical digest, OSA, Washington, DC, **56**, 403-404 (2001)
6. K. Koenig, I. Riemann, P. Fischer, and K. Halbhuber, "Intracellular Nanosurgery With Near Infrared Femtosecond Laser Pulses," Cell. Mol. Biol. **45,** 192-201 (1999)
7. U.K. Tirlapur, and K. Koenig, "Targeted transfection by femtosecond laser," Nature **448**, 290-291 (2002)
8. W. Watanabe, N. Arakawa, S. Matsunaga, T. Higashi, K. Fukui, K. Isobe, and K. Itoh, "Femtosecond laser disruption of subcellular organelles in a living cell," Opt. Express **12**, 18, 4203-4213 (2004), http://www.opticsexpress.org/abstract.cfm?URI=OPEX-12-18-4203

#6718 - $15.00 US Received 28 February 2005; revised 1 May 2005; accepted 2 May 2005

9. A. Vogel, and V. Venugopalan, "Mechanisms of Pulsed Laser Ablation of Biological Tissues," Chem. Rev. **103**, 2, 577-644 (2003)
10. M.W. Berns, J. Aist, J. Edwards, K. Strahs, J. Girton, P. McNeil, J.B. Rattner, M. Kitzes, M. Hammerwilson, L.H. Liaw, A. Siemens, M. Koonce, S. Peterson, S. Brenner, J. Burt, R. Walter, P. J. Bryant, D. Vandyk, J. Couclombe, T. Cahill, and G.S. Bern, "Laser microsurgery in cell and developmental biology," Science **213**, 505-513 (1981)
11. H. Liang, W.H. Wright, S. Cheng, W. He, and M.W. Berns, "Micromanipulation of Chromosomes in PTK2 Cells Using Laser Microsurgery (Optical Scalpel) in Combination with Laser-Induced Optical Force (Optical Tweezers), " Experimental Cell Research **204**, 110-120 (1993)
12. J.R. Aist, H. Liang, and M.W. Berns, "Astral and spindle forces in PtK_2 cells during anaphase B: a laser microbeam study," Journal of Cell Science **104**, 1207-1216 (1993)
13. S.W. Grill, J. Howard, E. Schäffer, E.H.K. Stelzer, and A.A. Hyman, "The Distribution of Active Force Generators Controls Mitotic Spindle Position," Science **301**, 518-521 (2003)
14. J. Noack, D.X. Hammer, G.D. Noojin, B.A. Rockwell, and A. Vogel, "Influence of pulse duration on mechanical effects after laser-induced breakdown in water," J. Appl. Phys. **83**, 12, 7488-7495 (1998)
15. C.B. Schaffer, J.F. Garcia, and E. Mazur, "Bulk heating of transparent materials using a high-repetition-rate femtosecond laser," Appl. Phys. A **76**, 351-354 (2003)
16. E.L.Botvinick, V.Venugopalan, J.V.Shah, L.H.Liaw, and M.W. Berns, "Controlled Ablation of Microtubules Using a Picosecond Laser," Biophys. J. **87**, 6, 4203-4212 (2004)
17. M.F. Yanik, H. Cinar, H.N. Cinar, A.D. Chisholm, Y. Jin, and A. Ben-Yakar, "Neurosurgery: Functional regeneration after laser axotomy," Nature **432**, 822 (2004)
18. C.S. Chen, M. Mrksich, S. Huang, G.M. Whitesides, and D.E. Ingber, "Geometric Control of Cell Life and Death," Science **276**, 1425-1427 (1997)
19. Y. Numaguchi, S. Huang, T.R. Polte, G.S. Eichler, N. Wang, and D.E. Ingber ,"Caldesmon-dependent switching between capillary endothelial cell growth and apoptosis through modulation of cell shape and contractility," Angiogenesis. **6**, 55-64 (2003)
20. S.H. Hu, J.X. Chen, and N. Wang, "Cell spreading controls balance of prestress by microtubules and extracellular matrix," Front. Biosci. **9**, 2177-2182 (2004)
21. F.J. Alenghat, S.M. Nauli, R. Kolb, J. Zhou, and D.E. Ingber, "Global cytoskeletal control of mechanotransduction in kidney epithelial cells," Exp. Cell Res. **301**, 23-30 (2004)
22. V. Venugopalan, A. Guerra, K. Nahen, and A. Vogel, "Role of Laser-Induced Plasma Formation in Pulsed Cellular Microsurgery and Micromanipulation," Phys. Rev. Lett. **88**, 078103, 1-4 (2002)
23. D. Gusnard, and R. H. Kirschner, "Cell and organelle shrinkage during preparation for scanning electron microscopy: Effects of fixation, dehydration and critical point drying," J. Microscopy **110**, 1, 51-57 (1977)
24. U. Brunk, V.P. Collins, and E. Arro, "The fixation, dehydration, drying and coating of cultured cells of SEM," J. Microscopy **123**, 2, 121-131 (1981)

1. Introduction

Ultrashort laser pulses are useful tools in biology in a variety of applications: first, to image cellular structures in microscopy [1-3]; second, to micromanipulate and dissect nanoscale structures in living cells and other biological materials [4-8]. When femtosecond laser pulses are focused by high numerical aperture objectives (NA>1), the laser radiation is confined to a very small focal volume, creating photon densities high enough to induce multiphoton absorption at the laser focus, even in normally transparent materials. This process, together with cascade ionization, generates very high concentrations of free electrons in the focal volume, resulting in plasma-mediated ablation of material [9]. There are two key advantages in using femtosecond lasers for bulk ablation of biological samples. First, the laser wavelength is centered in the near-infrared (around 800 nm) providing a high penetration depth in tissue. The nonlinear nature of the optical absorption makes it possible to treat any transparent sample, regardless of its linear absorption coefficient. Second, with a pulse duration of about 100 fs, only a few nanojoules of energy are necessary for material dissection [5,9] In contrast, green picosecond laser systems [10,11] and UV laser microscissors [12,13] require two to three orders of magnitude higher energy [14]. The low energy minimizes collateral damage in the vicinity of the laser focus and reduces the likelihood that the cell will be injured or killed.

Studies with glasses and soft materials have revealed that the extent of photodamage depends steeply on the incident laser pulse energy [15], but no comprehensive studies of the quantitative relationship between pulse energy and the extent of femtosecond laser ablation have been undertaken in biological samples. The dissection of isolated human chromosomes has been studied using atomic force microscopy (AFM) and fluorescence microscopy [6], but neither technique is a good measure of the removal of material from the bulk of the sample.

#6718 - $15.00 US Received 28 February 2005; revised 1 May 2005; accepted 2 May 2005

AFM examines only the surface of the sample and fluorescence microscopy cannot discriminate between photobleaching and material ablation. Because irradiation can alter the staining properties of the sample, restaining also does not allow differentiating between photo-induced chemical changes and removal of material [8]. A transmission electron microscopy (TEM) study confirms the cutting of microtubules using picosecond laser pulses of just a few nanojoules at 532 nm, but the authors noted a considerable amount of photobleaching [16]. Another recent publication on ablation of neurons in living C. elegans by highly focused fs-pulses (1.4 NA) shows photobleaching at pulse energies of 1–2 nJ [17]. However, the cuts in the neurons were performed at much higher energies of 10–40 nJ. Thus, for low-energy femtosecond pulses, the exact boundaries of photobleaching and material ablation have not been established.

To address this issue, we studied the effects of femtosecond laser irradiation in fluorescently-labeled structures in the cytoskeleton and nuclei of fixed cells using a combination of fluorescence microscopy and whole mount TEM. We used fluorescence microscopy to evaluate the extent of apparent photodamage, and TEM to determine the actual degree of material removal. Finally, we show that this technique can be applied to live cells by severing a single microtubule and leaving the rest of the microtubule network undisturbed.

2. Experimental methods

The laser radiation is generated in a custom-built chirped-pulse amplified titanium-sapphire laser system. A passively mode-locked oscillator delivers 100-fs pulses at a repetition rate of 80 MHz and a central wavelength of 790 nm. These pulses are regeneratively amplified to energies of up to 1 mJ at a repetition rate of 1 kHz. As these energies are far too high for subcellular ablation, we reduce the pulse energy to the nanojoule range with an attenuator. An adjustable neutral density filter wheel is used to regulate the energy at the sample. The laser light is focused into the sample with a 1.4-NA oil-immersion objective (Zeiss, Plan-Apochromat), leading to a theoretical spot size of roughly 340 nm. As the intense laser pulses experience group-velocity dispersion inside the microscope objective, the resulting pulse duration at the sample is approximately 200-250 fs [2]. The sample is placed on a piezo-controlled microscope stage that permits sample positioning with 10-nm precision along all three axes. A UV lamp (Osram, HB103 W/2) illuminates the sample and the emitted fluorescence is collected through the objective using a standard filter cube (FITC, Chroma Technology Corp.) and recorded with a CCD camera.

Bovine capillary endothelial cells (passage 10 to 15) were maintained at 37 °C in 10% CO2 on tissue culture dishes in a complete medium composed of low-glucose Dulbecco's modified Eagle's medium (DMEM; Gibco-BRL) supplemented with 10% fetal calf serum (FCS) (Hyclone), 10 mM HEPES (JRH-Biosciences), and glutamine (0.292 mg/ml)/penicillin (100 U/ml)/streptomycin (100 g/ml) as previously described [18].

For the live cell experiments, cells were transfected for 48 h with an adenoviral vector system [19,20] encoding enhanced green fluorescent protein (EGFP)-tagged G-tubulin, trypsinized (Trypsin–EDTA, Gibco), harvested, and seeded onto glass-bottomed 35 mm dishes (MatTek) in complete medium. Prior to imaging, cells were transferred into a nonfluorescent, CO_2-independent medium (pH 7.3) containing (in mM): $CaCl_2$ (1.26), $MgSO_4$ (0.81), KCl (5.36), KH_2PO_4 (0.44), NaCl (137), Na_2HPO_4 (0.34), D-glucose (5.55), L-glutamine (2.0), sodium pyruvate (1.0), HEPES (20.0), 1% bovine serum albumin, 10% calf serum, and MEM essential and nonessential amino acids (Sigma) [21].

For the fixed cell experiments, cells were then trypsinized (Trypsin EDTA, Gibco), harvested, and seeded either onto glass-bottomed 35 mm dishes (MatTek) or onto carbon-coated formvar on Embra TEM finder grids (Electron Microscopy Sciences) in complete medium. After allowing the cells to attach and spread for 12–24 hours, the cells were fixed in 4% formaldehyde (electron microscopy grade) in phosphate buffered saline (PBS) for 40 minutes, permeabilized in 0.1% Triton X-100 in PBS for 5 minutes, blocked in 1% bovine serum albumin in PBS for 1 hour, and stained for either actin (Alexa Fluor488 phalloidin, Molecular Probes) or nuclear DNA (Hoechst 33348, Molecular Probes), all at room

#6718 - $15.00 US Received 28 February 2005; revised 1 May 2005; accepted 2 May 2005

temperature. Afterwards the cells were stored and treated in an aqueous solution (PBS). Following laser treatment, cells were fixed in 2.5% glutaraldehyde in 0.1 M cacodylate buffer, pH 7.4, at 4 °C for one hour and then washed and stored in this buffer at 4 °C until processing. Prior to TEM imaging with a Philips CM-10 microscope, cells were fixed in 1% osmium tetroxide in 0.1 M cacodylate buffer, pH 7.4, at 4 °C for 30 minutes, washed in the same buffer, dehydrated in graded ethanol solutions, critical point dried, and carbon coated.

The TEM analysis gives a direct measure of the ablated area, as the electrons are sensitive to the amount of material they travel though. The ablated region appears lighter on the film, even if it is confined in the bulk of the sample. We took pictures of the cell samples at two different angles creating a stereoscopic image and then we measured the width of the ablated region averaging over three positions along the laser cut.

3. Results

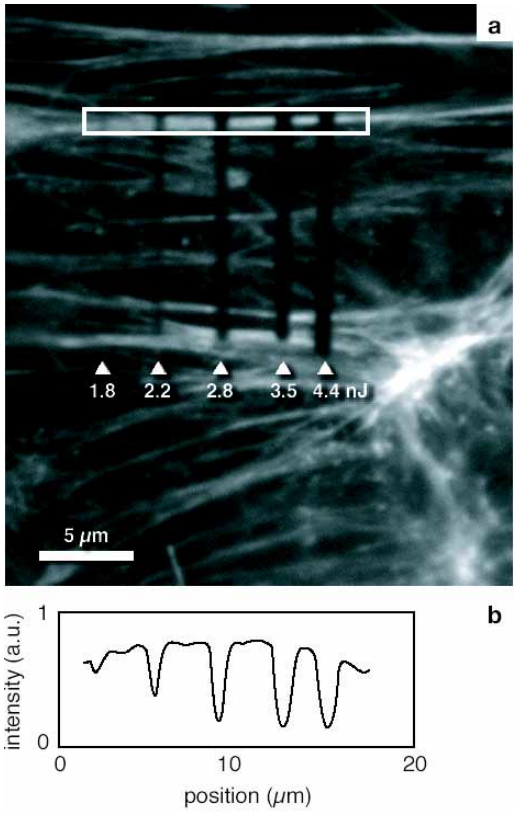

Fig. 1. (a) Cuts through fluorescently-labeled actin fibers in a fixed endothelial cell obtained by irradiation with femtosecond laser pulses of energies between 1.8 nJ and 4.4 nJ. (b) Fluorescence intensity profile along the actin bundle outlined in the image

Figure 1(a) shows the fluorescence from the actin network of a fixed endothelial cell after it has been irradiated along five parallel lines with various pulse energies. The sample was translated once per line at a speed of approximately 0.7 μm/s corresponding to roughly 15,000 pulses per line. Figure 1(b) shows that the fluorescence intensity following irradiation depends strongly on pulse energy. At 1.8 nJ the effect of irradiation is barely visible in the fluorescence image. Increasing the pulse energy to 2.2 nJ produces a clear dip in fluorescence with a width of 240 nm at FWHM. At higher energy the FWHM-width of the dip in fluorescence scales with pulse energy, from 360 nm at 2.8 nJ, to 500 nm at 3.5 nJ and 600 nm at 4.4 nJ.

#6718 - $15.00 US Received 28 February 2005; revised 1 May 2005; accepted 2 May 2005

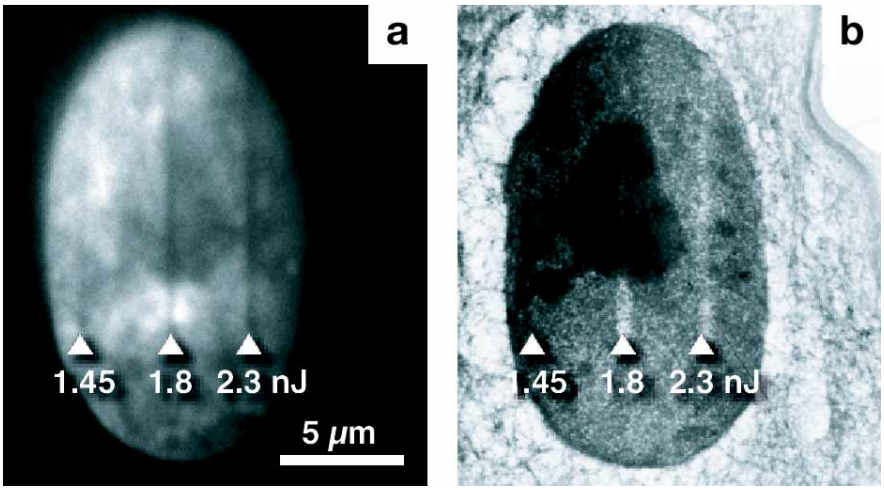

Fig. 2. Cuts in the nucleus of a fixed endothelial cell at various laser energies, imaged by (a) fluorescence microscopy and (b) electron microscopy.

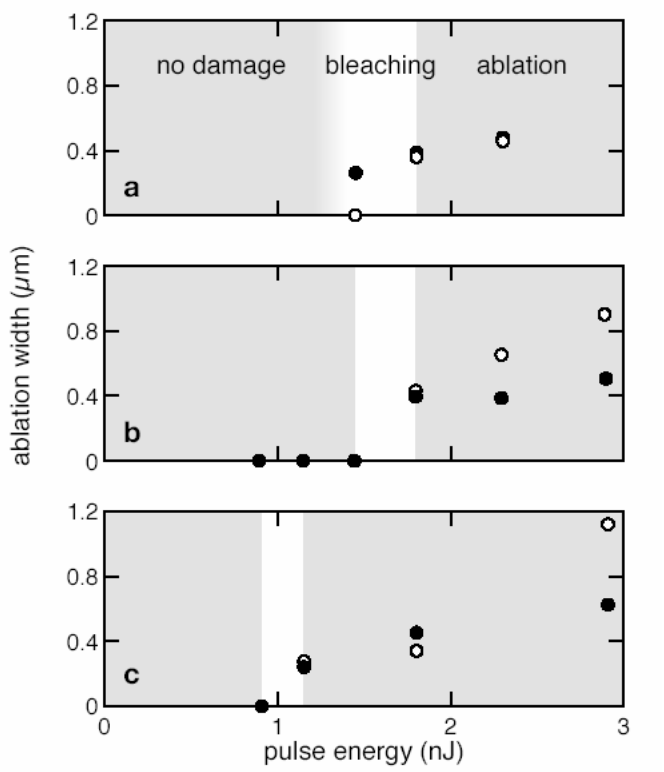

Fig. 3. Pulse energy dependence of the ablation width of cuts in the nucleus of endothelial cells measured by fluorescence microscopy (filled circles) and TEM (open circles) in three different cells (a)–(c).

#6718 - $15.00 US
Received 28 February 2005; revised 1 May 2005; accepted 2 May 2005

Figure 2 shows that loss of fluorescence does not always correspond to removal of material. The figure shows both fluorescence and TEM images of the nucleus of the same fixed endothelial cell after irradiation at three different energies. While a slight loss of fluorescence can be observed for a pulse energy of 1.45 nJ, the TEM image shows no material removal. The loss of fluorescence must thus be due to photobleaching. At higher energies we see clear "cuts" in both images.

Figure 3(a) shows the dissection width of the cuts observed in Fig. 2. The data allow us to define three regimes of irradiation: no interaction (no damage visible in either image), photobleaching without material loss (only the fluorescence image shows a change), and removal of material (both images show cuts). Figure 3(b) and 3(c) show similar data obtained in the nuclei of two other cells. In each case, irradiation at pulse energies below 1 nJ causes no change in either image, while energies above 1.7 nJ do cause changes in both images. Thus, the threshold energy for plasma-mediated ablation falls between 1–1.7 nJ. For pulse energies above 10–15 nJ, a much larger part of the cell is ablated (not shown). This phenomenon is most likely due to cavitation, which has been observed during laser irradiation of water, soft materials, and biological tissues [14,22]. Part of the energy delivered to the sample cannot be dissipated through thermal diffusion, producing a rapid, local increase in material temperature, leading to an explosive expansion of the material and, thus, damage far from the laser focus.

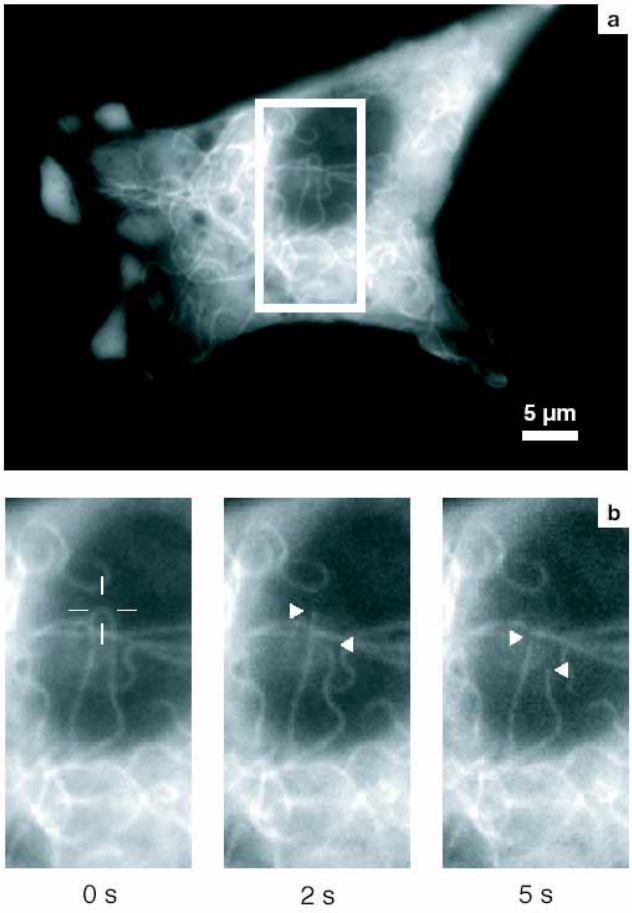

Fig. 4. (a) Fluorescence microscope image of GFP-labeled microtubule network in an endothelial cell. (b) time-lapse sequence showing rapid retraction of microtubule due to depolymerization. The cross hair shows the position targeted by the laser; the triangles show the retracting ends of the microtubule.

#6718 - $15.00 US Received 28 February 2005; revised 1 May 2005; accepted 2 May 2005

While the thresholds in Fig. 3 vary from sample to sample, the energy threshold of ablation is at most 20% higher than the photobleaching threshold. In other words, at energies exceeding 1.2 times the threshold for which fluorescence disappears, one can be assured of material removal. The TEM and fluorescence microscopy measurements reveal that the plasma-mediated ablation width depends strongly on pulse energy, with pulse energies between 1.2 and 1.7 nJ producing material loss as small as 200 nm (Figs. 3(a) and 3(c)). Above 1.7 nJ, the dissection width increases with energy; around 3 nJ the width is approximately one micrometer. At higher pulse energies, the dissection widths obtained from the TEM images are consistently larger than those obtained from the fluorescence images. This discrepancy is likely due to the TEM sample processing. Post-fixation, dehydration and critical point drying have all been shown to cause shrinkage in cellular contents while maintaining the usual structural relationship of components within the cell [23,24]. This shrinkage can result in a retraction of cellular material away from the ablated area, thus enlarging the ablation zone in the cells subsequently viewed by TEM. The TEM data in Figure 3 therefore likely overestimate the extent of laser induced material removal.

To show the spatial selectivity of femtosecond laser nanosurgery in cells we targeted microtubules in live cells. The microtubule network is sensitive to external disruptions and can be used as good indicator for the extent of damage induced by the laser irradiation outside the focal volume. Figure 4(a) is a fluorescence microscope image of a live bovine endothelial cell whose microtubules express green fluorescent protein. The dark region in the middle of the cell is the nucleus. We severed a bent region of a single microtubule located above the nucleus using about 1000 laser pulses with an energy of 1.5 nJ. The curved end of the microtubule immediately recoiled to a straight configuration within the first 2 s after laser ablation, indicating the release of stored elastic energy in the molecular filament; this was immediately followed by depolymerization of the cut ends of microtubule due to release of tubulin monomers, as shown in time-lapse frames in Fig. 4(b). The neighboring microtubules, which are less than 1 μm away, remain undisturbed. Even though it is impossible to get a measure of the exact size of the laser dissection in this type of live cell experiment, the narrow confinement of plasma-mediated laser ablation confirms the TEM data obtained for fixed cells.

4. Conclusion

The use of ultrashort laser pulses for dissecting and imaging cells and subcellular structures in cellular and developmental biology is increasing rapidly. In this report we presented a first systematic study of the relationship between pulse energy and subcellular material loss using femtosecond laser pulses. We used a combination of fluorescence and electron microscopy to establish the thresholds for fluorescence photobleaching and material removal under tight focusing conditions. The results presented here show that there is a range of energy for which photobleaching occurs without ablation. We find that the optimal energy range for plasma-mediated ablation is from about 20% above the photobleaching threshold to about 3 nJ. In this range, one is assured of dissection with a resolution as small as 200 nm. At higher energies the size of the dissected region increases rapidly with laser pulse energy. We also demonstrated that this technique can be successfully applied to live cells with high spatial resolution. These results will help guide and interpret femtosecond laser material removal and real time fluorescence imaging to investigate cell structure and function at increasingly small length scales.

Acknowledgments

We would like to acknowledge support from the German Research Foundation (DFG), the NCI program “Nuclear Structure and Cancer”, the National Science Foundation (NSF), the National Institutes of Health, NASA, and the NSF-sponsored MRSEC at Harvard University